

Chapter 7

Simulated Performance of Integrated Tracking System

7.1 Introduction

In this section we describe the performance of the CDF integrated tracking system for Run II. This includes the new central tracker, COT, and the new silicon vertex detectors, SVX II+ISL.

In Section 7.2 we describe the simulation tools used for evaluating the performance of COT and SVX II. In Section 7.3 we define the data sample used to measure tracking performance of COT and SVX II. In Section 7.4, we describe how the performance of the COT in Run II can be gauged from the performance of the CTC in Run I, along with the simulation results. In Section 7.5, we demonstrate the performance of the combined SVX II and ISL system. In Section 7.6 we study the performance of the combined system: COT+ISL+SVX II. Section 7.6.1 outlines a method used to link tracks in the inner detector (i.e. SVX+ISL) to the COT, in the r - ϕ plane. We describe an algorithm developed for linking hits in the r - z plane in Section 7.6.2. Finally, in Section 7.6.3, we study the helix parameter resolution of the integrated tracker, as a function of luminosity.

7.2 Simulation of COT, ISL and SVX II

The COT simulation is a modification of the current full CTC simulation. It uses the correct COT geometry (e.g. the cell sizes, the different tilt of the cells, etc.) and incorporates the predicted pulse width and drift velocity. The single hit resolution is based on experience with the CTC and is a conservatively chosen to 200 μm .

For the SVX II we use a simulation which is an extension of our present full SVX' simulation. It in-

corporates the fifth additional layer, the stereo layers, and the ambiguity in the 90° layers.

For the ISL, we use a simple simulation that generates hits by recording Monte Carlo track positions at the ISL radii. We then use a parameterization of the detectors' hit resolutions to study the helix fit resolutions of reconstructed tracks.

7.3 Data Sample

We have chosen tracking of b -daughters in $t\bar{t}$ events as the benchmark for the performance of the tracking system. This is one of the most important and challenging environments in which one needs to find tracks efficiently. The generator used is the HERWIG Monte Carlo. It is essential to understand the effects of multiple interactions (see Figure 1.1). Therefore, we have developed a procedure for mixing one $t\bar{t}$ event with any number of generated minimum bias events. The minimum bias Monte Carlo has been tuned to reproduce the observed multiplicities in CDF data. For these tracking studies, we use Monte Carlo data samples with $t\bar{t}$ events alone, one $t\bar{t}$ event with a mean of three underlying minimum bias events, or one $t\bar{t}$ event with a mean of six underlying minimum bias events. The actual number of underlying minimum bias events for each $t\bar{t}$ event is drawn from a Poisson distribution with the appropriate mean. The $t\bar{t}$ -alone dataset corresponds to low luminosity, while the three overlaid minimum bias event sample corresponds to $\mathcal{L} = 1(3) \times 10^{32} \text{cm}^{-2} \text{s}^{-1}$ for 36 (108) Tevatron bunches, and the six overlaid minimum bias event samples corresponds to $\mathcal{L} = 2(6) \times 10^{32} \text{cm}^{-2} \text{s}^{-1}$ for 36 (108) Tevatron bunches, respectively.

7.4 COT performance

We begin by modeling the COT as a stand-alone tracker. Two approaches are used to understand its performance. First, we rely on the nine years of experience with the CTC and the fact that the COT is very similar in design. The pattern recognition algorithms and performance of the CTC in the Tevatron environment are well understood. From scaling arguments, we can compare the performance of the CTC at Run I luminosities with the performance of the COT at Run II luminosities. This gives us a data-driven prediction of the COT performance. However, this projected performance is a lower limit since the COT has twice as many stereo measurements and better two-track resolution than the CTC. The second technique uses a simplified pattern recognition procedure to evaluate the COT performance. This approach has the advantage that it can be used for stand-alone studies of the COT as well as integrated studies of the COT and SVX II+ISL.

7.4.1 Projected COT performance based on CTC data

We characterize tracking chamber performance with momentum resolution, impact parameter resolution and tracking efficiency for daughter tracks from B hadrons from top quark decays. At $\mathcal{L} = 1 \times 10^{31} \text{cm}^{-2}\text{s}^{-1}$ in Run I, we measured the CTC (stand-alone) momentum resolution as $\delta p_T/p_T^2 = 0.2\%$, and the impact parameter resolution as $\approx 340 \mu\text{m}$. We measured the efficiency for b-daughter tracks from top quark decays by superimposing a Monte Carlo track, with the expected p_T and $\Delta R(\text{track-jet})$ given by HERWIG, onto a jet from the data and re-tracking the event. At $\mathcal{L} = 1 \times 10^{31} \text{cm}^{-2}\text{s}^{-1}$, the CTC efficiency was measured to be 94.6%.

As noted above (and described in detail in Section 4.7.3), the performance of the COT in Run II can be gauged from the performance of the CTC in Run I, by simple scaling arguments based on the chamber geometries, pulse shaping, drift velocities, and the number of Tevatron bunches. In many ways this is the *most* reliable predictor of minimum COT performance because it is based on real data, mature reconstruction code, and simple scaling principles. This scaling suggests that the performance of the axial layers of the CTC at $\mathcal{L} = 1 \times 10^{31} \text{cm}^{-2}\text{s}^{-1}$, is equivalent to the performance of the axial and stereo layers of

the COT at $\mathcal{L} = 7.6 \times 10^{31} \text{cm}^{-2}\text{s}^{-1}$ (36 bunches) and $\mathcal{L} = 1.9 \times 10^{32} \text{cm}^{-2}\text{s}^{-1}$ (108 bunches). On the basis of these arguments alone we can predict high tracking efficiency and good momentum resolution for the COT in Run II.

7.4.2 Pattern Recognition in COT

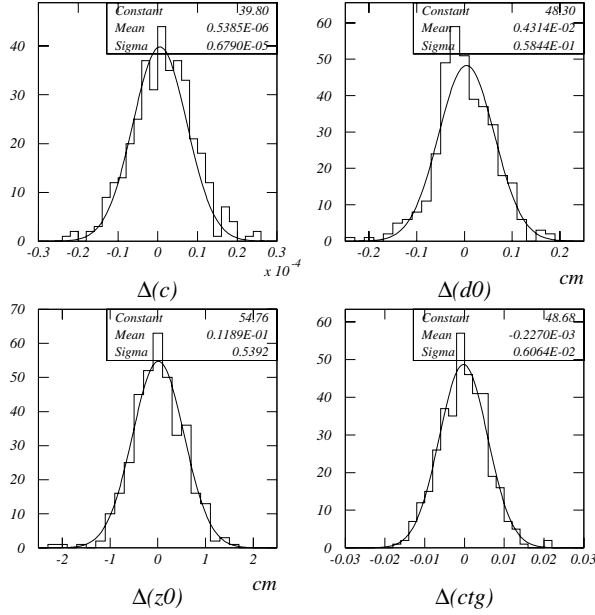
Our experience with the CTC has taught us that tracking chambers of this design are extremely efficient for single wire hits, so, strictly speaking, track finding should not be a problem. The tracking inefficiency in the CTC was due to attaching wrong hits to tracks and hence pulling the fitted helix from the correct one. The information is there, but the tracks are “lost” to mismeasurement.

Since the COT and CTC have similar $r\text{-}\phi$ characteristics, we expect their pattern recognition problems to be similar. We have studied hit availability in the COT and “confusion” at high luminosity using tools developed with the CTC. For these studies a Monte Carlo track is simulated and hits are created on the chamber wires according to the track’s helix parameters and the resolution of the COT. The challenge of finding the track, with the correct p_T , impact parameter, ϕ_0 , etc., is the selection of the *correct* hits to use in the helix fitting procedure. To analyze our ability to do so in the COT under Run II conditions, we use the following procedure:

1. From the momentum of the generated particle in the Monte Carlo, we calculate the corresponding helix parameters. These helix parameters are then used to open a 1 mm wide road, in both $r\text{-}\phi$ and $r\text{-}z$.
2. All hits within the road are picked up and fed to the same helix fitting routine which we used in the Level 3 trigger of Run I. This is a sophisticated routine which adds and/or rejects hits based on the χ^2 of the fit.
3. The returned helix parameters are compared with the input track parameters to measure the p_T resolution (curvature), impact parameter resolution, z_0 resolution, and $\cot(\theta)$ resolution.

This procedure is performed on the $t\bar{t}$ plus minimum bias event samples to examine the performance of the COT under different Tevatron conditions. The results of these studies are summarized below.

COT Resolutions: Top b -daughters



COT Resolution Vs. Luminosity

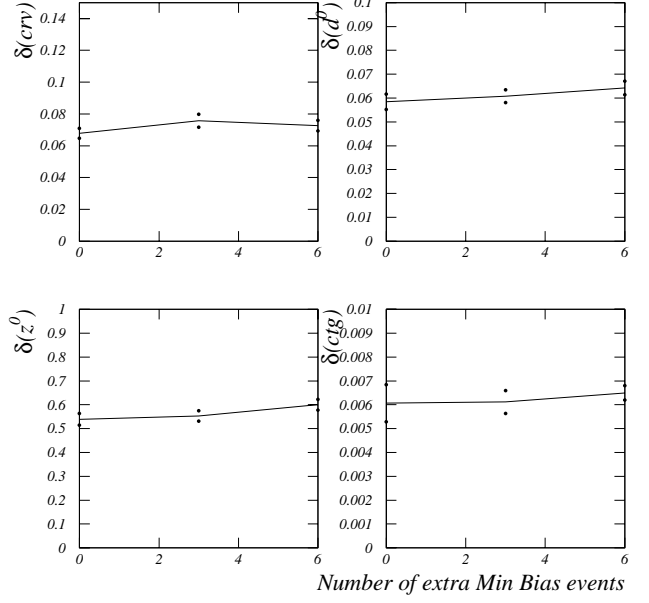


Figure 7.1: Left: Helix parameter resolutions at low luminosity. Right: Helix parameter resolutions versus the mean number of extra minimum bias events

7.4.3 COT Simulation Results

On the left in Figure 7.1 we show the resolution of the reconstructed curvature, impact parameter, z_0 and $\cot\theta$ from COT tracking for low luminosity.

The resolution is defined as the difference between the reconstructed parameter and the helix parameters calculated from the trajectory of the generated particle. The resolution on the curvature is $0.68 \times 10^{-4} \text{ cm}^{-1}$ which corresponds to a momentum resolution of $\delta p_T/p_T^2 \simeq 0.3\% (\text{GeV}/c)^{-1}$. The impact parameter resolution for the COT alone is about $600 \mu\text{m}$ while the z_0 resolution is about 5 mm and the $\cot\theta$ resolution is 6×10^{-3} .

These numbers agree with our expectations for COT performance given the larger inner radius of COT compared to CTC.

Although a single $t\bar{t}$ event represents a busy tracking environment, unless several minimum bias events are overlapped with this event, it still does not represent the operating conditions of Run II. Therefore, we have studied the effect of multiple interactions on the resolution of the tracking parameters. The right plot of Figure 7.1 shows the dependence of the resolution of the reconstructed curvature, impact parameter, z_0 and $\cot\theta$ on the mean number of extra minimum bias events for means of 0, 3, and 6 extra minimum bias

COT Momentum resolution Vs. P_T

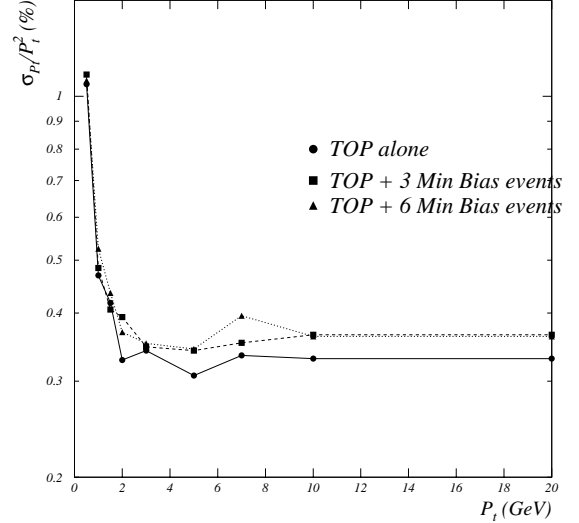


Figure 7.2: Momentum Resolution versus p_T for three luminosities.

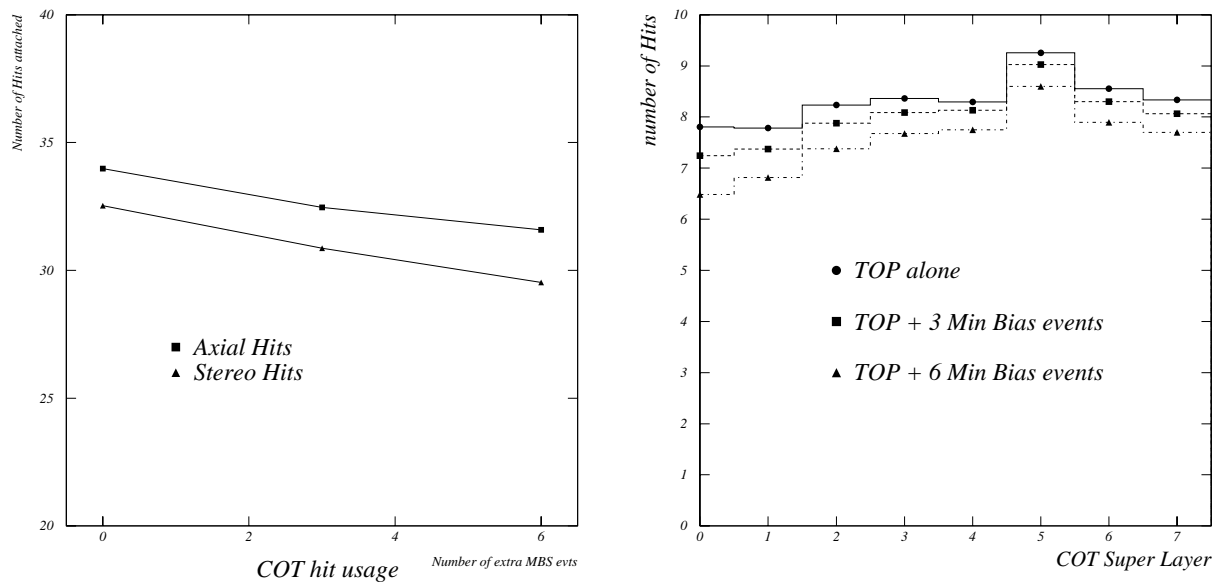


Figure 7.3: Left: Hit usage in COT versus mean number of overlapped minimum bias events. Right: Hit usage in COT versus super-layer for three different instantaneous luminosities.

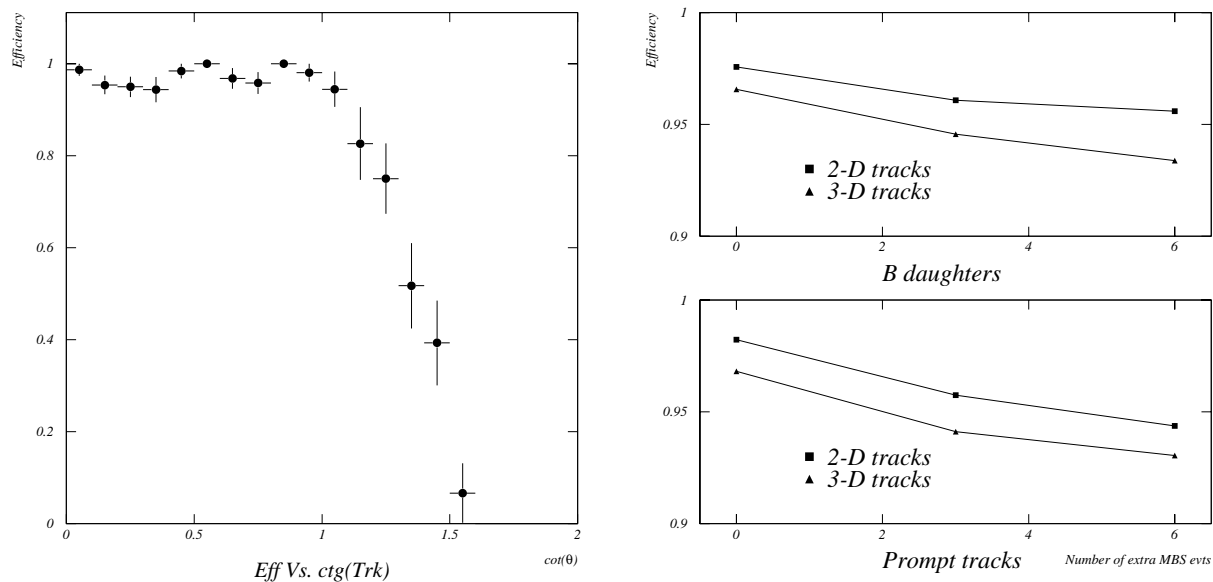


Figure 7.4: Left: Tracking efficiency versus $\cot \theta$ for prompt tracks at low luminosity in the COT. Right: COT track finding efficiency versus mean number of overlapped minimum bias event. The upper plot is for tracks from B meson daughters from $t\bar{t}$ decays, and the lower for prompt tracks.

events. The dots in Figure represent the 1σ uncertainty on the resolution measurement, note that some of the apparent performance variation with luminosity is nothing more than our Monte Carlo statistics! Recall that 6 extra minimum bias events corresponds to a luminosity of $6 \times 10^{32} \text{ cm}^{-2} \text{ s}^{-1}$ for 108 bunch operation. We see very little degradation of the COT performance with increasing luminosity.

We have also explicitly measured the p_T resolution versus track p_T (Figure 7.2) for the three different data samples and only a slight dependence on luminosity is observed.

High quality tracks typically use a large number of hits that have passed strict selection requirements. As the tracking environment becomes more confused, fewer hits may be used for track fitting. The left plot in Figure 7.3 shows the average number of axial and stereo hits attached to a track as a function of the number of underlying minimum bias events. Note that the maximum possible number of hits is 48 each for both axial and stereo measurements but the strict hit selection in the fitting procedure reduces the number of hits actually used. The reduction in hit usage from low luminosity to the equivalent of $6 \times 10^{32} \text{ cm}^{-2} \text{ s}^{-1}$ with 108 bunches, is modest; as seen in the right hand plot, the loss occurs mainly in the inner COT layers. Reduced performance caused by lost hits in the inner super-layers will be regained partially through the integrated use of the ISL and SVX II in the pattern recognition.

Besides excellent resolution on found tracks, it is essential that we have high efficiency for identifying tracks. We define the tracking efficiency as the fraction of tracks found with all of the helix parameters within five standard deviations of the correct value as defined by the Monte Carlo track. The standard deviation of a parameter is fixed to its value at low luminosity, shown in Figure 7.1. We measure the track finding efficiency both for prompt tracks and for tracks of B meson daughters from top quark decays. The tracking efficiency as a function of $\cot \theta$ for prompt tracks is shown in Figure 7.4. It is flat out to $\cot \theta=1$ after which the track no longer goes through all super-layers.

In Figure 7.4 we also show the efficiency as a function of the mean number of underlying minimum bias events. Earlier, we used scaling arguments to predict a COT efficiency for B meson daughters of 94.6% at a luminosity $7.6 \times 10^{31} \text{ cm}^{-2} \text{ s}^{-1}$ with 36 bunches. This corresponds to 2.4 underlying minimum bias events,

where we measure now about 95% for 3-D tracks. Once again the performance of the COT with increasing luminosity does not degrade significantly and the slight degradation will be recovered by integrating the ISL and SVX II into the pattern recognition.

7.5 SVX II+ISL performance

In this section we describe the stand-alone performance of the “inner tracking” system of SVX II + ISL. This is of primary importance for tracking in the plug region, $1.0 < |\eta| < 2.0$, where there is little or no COT coverage, and it is also essential for integrated SVX II+ISL+COT tracking in the central region, $|\eta| < 1.0$.

7.5.1 r - ϕ Tracking

Ultimately, we will find track segments in the full seven layers of SVX II+ISL and link these to track segments found in the COT super-layers. However, for these studies we combined a full SVX II hit level simulation and pattern recognition with a simple ISL simulation and studied the power of the SVX II+ISL combination by projecting the SVX II tracks to the ISL radii and looking at hit matching.

7.5.1.1 SVX II r - ϕ Tracking

We first reconstruct tracks in the five layers of SVX II. The pattern recognition requires at least four hits to define a track.

The probability of a particle depositing four or more hits in the SVX II is 95% due to hits lost in interbarrel gaps. In order to remove effects due to SVX II length, this study considered only events with a primary vertex at $|Z| \leq 45 \text{ cm}$.

Fake tracks are combinations of hits from several different tracks, so these hits are “shared” by two or more tracks. We use a pruning algorithm which discriminates against shared hits and increases the purity to S:N $\sim 4.5:1$ while maintaining an efficiency of $\sim 93\%$.

The tracking efficiency is shown as a function of p_T and $|\eta|$ in Fig. 7.5. It is flat in p_T and flat in $|\eta|$ up to ~ 2 .

The helix parameter resolutions of the 2D tracks found in SVX II are shown in Fig. 7.5. The distributions are not well fit by a single gaussian because they are a mix of 4 and 5 hit tracks. The transverse

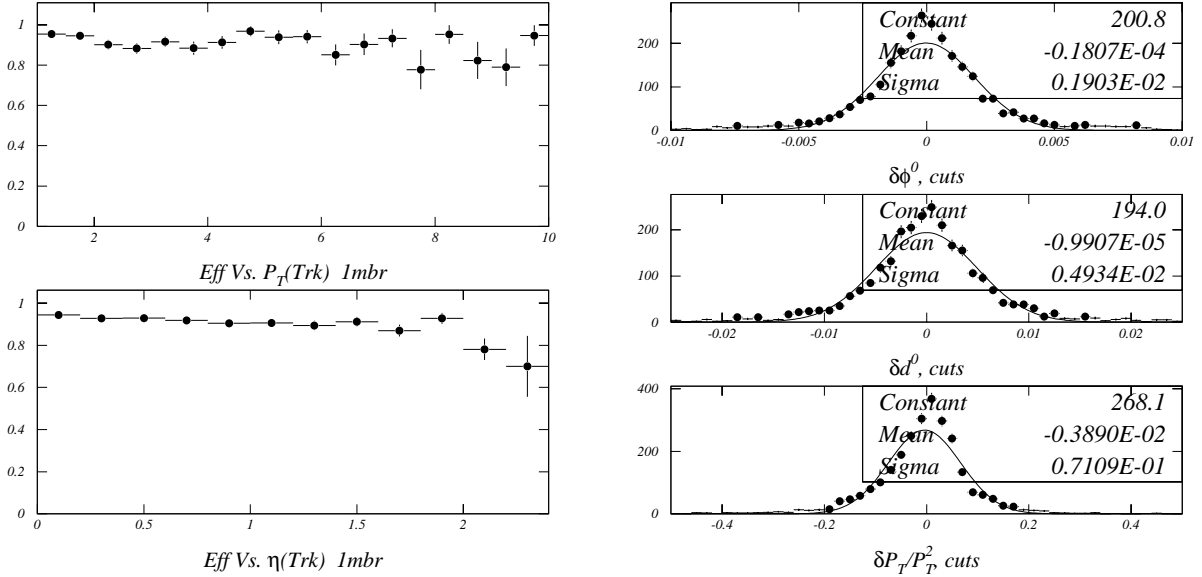


Figure 7.5: Left: The efficiency of finding r - ϕ tracks with the SVX II stand-alone pattern recognition and pruning is shown as a function of p_T and $|\eta|$ for b daughters in top + 1 minimum bias events. Right: The 2D helix parameter resolutions obtained with SVX II stand-alone tracks.

momentum resolution is $\delta p_T/p_T^2 \sim 7\%$. The impact parameter resolution is $\sim 50 \mu\text{m}$ and is dominated by the projection uncertainty that arises from the p_T resolution.

While the five layer SVX II can find 2D tracks with high efficiency it has the following shortcomings:

- low track purity (see below)
- poor resolution (p_T and impact parameter).

These limit the ability to link to COT, perform b-tagging, and identify leptons using track matching to a muon/electron tower. Additional information from ISL layers at larger radii is essential to:

- reject ghost tracks
- improve the p_T and hence the impact parameter resolution.

7.5.1.2 ISL hit matching

To evaluate the rejection power of a single ISL layer, we compute the distance between the extrapolated SVX II track and the nearest hit in the ISL layer at 20 cm. This is shown on the left in Figure 7.6 (open histogram). The bulk of nearest hits are correct hits, with an extrapolation accuracy of $50 \mu\text{m}$. The fraction of the cases in which the nearest hit *does not*

belong to the track is $\sim 5\%$ (shaded histogram). For those cases the difference between the nearest hit and the correct hit is shown on the right. About a third of the time, the nearest hit and the correct hit are within $220 \mu\text{m}$ of each other. Since the readout pitch is $110 \mu\text{m}$, hits this close together would in fact be merged into a single wide hit. It is only the remaining 3% of tracks which will lead to hit assignment ambiguity. Performing a fit which includes the outer layers will reduce the effects of multiple scattering, the combinatorics, and the effects of residual hit ambiguities from the sixth layer. ISL hit matching improves the track purity. For example, even a crude procedure such as requiring that the nearest hit be within 2.5 mm of the SVX II projection (i.e. full scale in Figure 7.6) improves the purity to S:N = 12:1, with high efficiency.

7.5.2 r - z Tracking

We will show in section 7.6.2 that completing the stereo in the central region with the coverage of the full tracking system is straightforward. For tracking in the plug region without COT, the stereo must be completed using SVX II and ISL alone.

Requiring three out of the four small angle stereo layers in SVX II+ISL, will yield high efficiency and

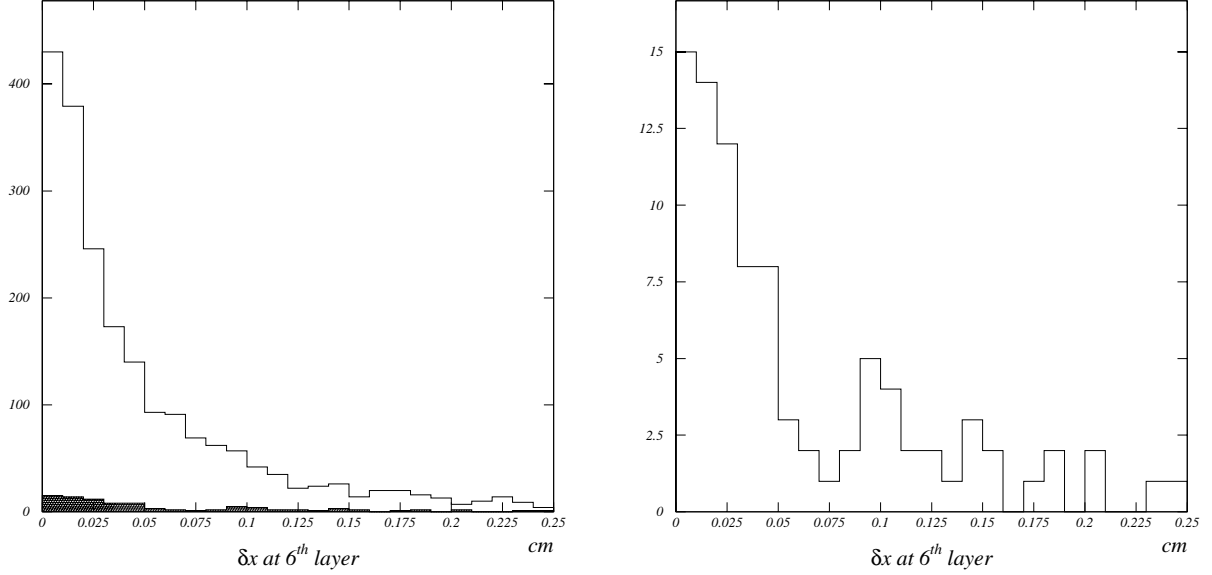


Figure 7.6: Left: The distance between the SVX II projection and the nearest ISL hit at $r = 20$ cm. The open histogram is for all hit combinations. The shaded histogram shows the cases where the nearest hit is not the correct hit. Right: The distance between the ISL hit which is nearest the SVX II projection and the correct hit is plotted for cases in which the nearest hit is *not* the correct hit

still provide z_0 resolution similar to that obtained with the CTC in Run I. It suffices to associate the track with its primary vertex, since all primary vertices will already have been found with high precision using SVX II's 90° stereo layers. Using the precise Z_{vertex} information, with the SVX II+ISL small angle stereo, one can attach the 90° hits in SVX II, and improve the final $\cot\theta$ and z_0 resolutions enough to allow for 3D vertexing.

7.5.3 Resolution of SVX II+ISL System

Once the tracks have been found, the precision space points and long lever arm provided by SVX II and ISL will yield excellent resolution on the helix parameters since the p_T resolution depends on the square of the lever arm. We have studied this with a parameterization of the detector resolutions. As shown in Figures. 7.7 and 7.8, we obtain the following asymptotic resolutions for the forward barrel (two ISL layers at $r = 20$ and 28 cm):

- $\delta p_T / p_T^2 \sim 0.4\%$
- $\delta d_0 = 15 \mu\text{m}$
- $\delta\phi_0 = 0.3 \text{ mrad}$

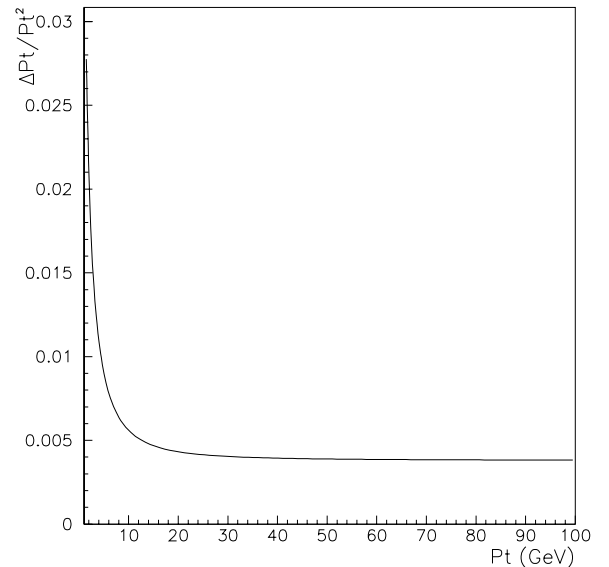


Figure 7.7: The p_T resolution obtained from a parametrization of the ISL resolution is plotted as a function of p_T .

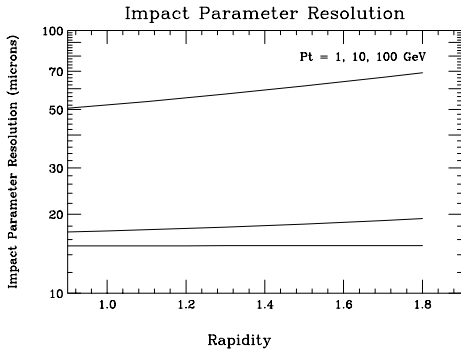


Figure 7.8: The impact parameter resolution obtained from a parameterization of the ISL resolution is plotted as a function of $|\eta|$.

Detector Configuration	Single tag eff.(%)	Double tag eff.(%)
SVX'+CTC	37.6 ± 1.0	6.9 ± 0.5
SVX II+COT	46.7 ± 1.1	8.7 ± 0.6
SVX II+ISL+COT	60.1 ± 1.0	15.1 ± 0.8

Table 7.1: Efficiency for single and double b-tagging in $t\bar{t}$ Monte Carlo for different detector configurations. The results are from a parametric study.

The p_T resolution is within a factor of two of that obtained with the full CTC in Run I and is sufficient for track matching and E/p cuts for electron and photon identification in the plug calorimeter. It will also enable *in situ* calibration of the plug calorimeter energy scale.

The impact parameter resolution is about what was obtained with the CTC+SVX in Run I. It will extend our b-tagging capabilities into the plug region, $|\eta| < 2.0$.

7.5.4 b-tagging for $|\eta| > 1$

We have carried out a parametric study of the b-tagging efficiency with SVX II+ISL. Beginning with generator level 4-vectors, we apply detector acceptance cuts and tracking efficiencies for SVX II, ISL, and COT. Helix parameter smearing is done based on the expected resolutions and the resulting tracks are fed to a vertex fitter to perform two dimensional secondary vertex tagging. The results are shown in Table 7.1. Of most significance is the factor of two

increase in double tag efficiency over the Run I configuration. This results from the extension of precision tracking to $|\eta| \sim 2$. This will have a significant impact on the top mass measurement since some of the systematic uncertainties are reduced in double tagged events. It should also allow studies of single top production for which the b quarks tend to be more forward.

7.5.5 Pointing into COT

The SVX II+ISL combination can find tracks efficiently, with high purity, and with good resolution. An added benefit of the integrated silicon tracker is the possibility of using these tracks as an integral part of the overall track reconstruction with the COT. This is especially important in the region $|\eta| > 1$ in which the COT coverage is incomplete. Even if the number of COT super-layer segments is too small to efficiently find full COT tracks with high efficiency, the SVX II+ISL tracks have sufficient pointing resolution to match to the COT segments in the inner super-layers. This can improve the momentum resolution and help in the stereo reconstruction.

The pointing uncertainties at various radii are shown in Table 7.2 for tracks of various momenta (multiple scattering is included assuming normal incidence). Note that for $p_T \geq 3$ GeV, the pointing resolution of the SVX II and just the single ISL layer at $r = 22$ cm is smaller than the COT cell size (7.6 mm) even at the radius of the outer super-layer. If a hit from the outer ISL layer is included (Table 7.2C), the pointing resolution at the inner COT super-layers ($r = 60$ cm) is comparable to the COT hit resolution, and the combination of the COT information with the SVX II+ISL track will improve the resolution considerably. This allows a completely different approach to integrating the inner and outer tracking chambers as discussed below.

7.6 Integrated Tracking Performance (SVX II+ISL+COT)

The procedure used during Run I to link SVX' hits with CTC tracks worked as follows: For a given CTC track, we extrapolated the helix to the outermost layer of the SVX' and performed a tree search within a road defined by the CTC track. SVX' hits were attached to the CTC track based on the combined χ^2 . Naturally, this method cannot add efficiency; it may

A: SVX II			
Radius	$p_T = 1$ GeV	3 GeV	10 GeV
20 cm	0.24 mm	0.16 mm	0.15 mm
30 cm	0.84 mm	0.53 mm	0.48 mm
80 cm	9.5 mm	5.5 mm	5.0 mm
130 cm	27.5 mm	16.0 mm	14.0 mm

B: SVX II+ISL ($r = 22$ cm)			
Radius	$p_T = 1$ GeV	3 GeV	10 GeV
30 cm	0.15 mm	0.06 mm	0.04 mm
80 cm	3.4 mm	1.3 mm	0.73 mm
130 cm	11.0 mm	4.0 mm	2.3 mm

C: SVX II+ISL ($r=28$ cm)			
Radius	$p_T = 1$ GeV	3 GeV	10 GeV
60 cm	0.9 mm	0.3 mm	0.2 mm
80 cm	2.0 mm	0.7 mm	0.4 mm
130 cm	6.7 mm	2.5 mm	1.3 mm

Table 7.2: Pointing resolutions at various radii are shown for tracks of various momenta. The upper table (A) is for SVX II alone. The middle table (B) is for SVX II plus the central ISL layer at $r = 22$ cm. The lower table (C) is for SVX II plus both of the forward ISL layers ($r = 20$ cm and $r = 28$ cm).

only improve the resolution of already found CTC tracks.

This approach represents a minimal baseline algorithm which we understand very well. However, the additional layers of ISL when combined with SVX II, allow implementation of stand-alone silicon based track finding algorithms. These algorithms will substantially improve tracking performance in Run II.

7.6.1 Linking COT with SVX II+ISL: r - ϕ

The algorithm described below uses line segments from the SVX II+ISL+COT system. These line segments are obtained from five axial “super-layers” (four in the COT and one from the SVX+ISL system). The line segments in the various super-layers are then linked to form tracks using the position and direction of the lines.

To evaluate the performance of this algorithm we define line segments as follows:

- **COT**

In each axial super-layer the position and direction of a Monte Carlo generated particle is

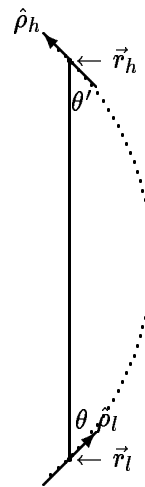


Figure 7.9: Geometry used for line-to-line linking.

smearred by the single hit resolution using the number of un-obscured hits present in the detector.

- **SVX II+ISL**

We use the reconstructed tracks found in the SVX II+ISL system (see Section 7.5).

For line-to-line linking we parameterize the lines by their position and direction at the super-layer center, $\vec{r}_{l,h}$ and $\hat{\rho}_{l,h}$ where the index l and h refer to the inner and outer line. Matching is by angle as shown in Figure 7.9: angles θ and θ' should match. A cut is put at

$$|\sin \Delta\theta| < 0.025 \quad (7.1)$$

If more than one outer line matches an inner line (or vice-versa) using the cut above, the links with the lowest $|\sin \Delta\theta|$ are kept and links are stored in both directions, outer to inner and inner to outer. Figure 7.10 shows the result of linking super-layers 7 and 5 within the COT, as well as super-layer 7 and the SVX II+ISL. From this figure we conclude that even in a complicated b-jet from top decay, the line segments can be matched correctly with low fake rates.

We studied the efficiency of this procedure and found the individual line segment linking efficiency to be high. For example: linking super-layers 7 and 5 is $\sim 99\%$ efficient whilst super-layer 7 and the SVX II+ISL is $\sim 92\%$ efficient. As a result the overall track reconstructing efficiency using all available combinations is expected to be very high.

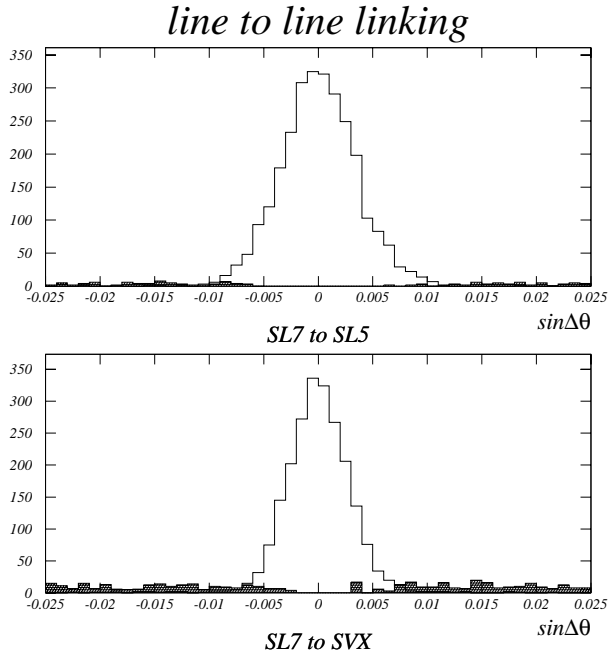


Figure 7.10: $\sin \Delta\theta$ distribution for the correct match and for spurious matches (hashed) is shown for top: super-layers 7 and 5 within COT, and bottom: super-layer 7 in COT and SVX II+ISL

It is also instructive to note that the quality of the links between COT super-layer 7 and SVX II+ISL, is better even than that to the nearby COT super-layer 5. This implies that even for large η , this procedure will allow matching of SVX II+ISL tracks to the available information in the COT. The COT measurements would substantially extend the lever arm and correspondingly improve the momentum resolution for such tracks.

7.6.2 Linking COT with SVX II+ISL: r - z

Since both SVX II and ISL are 3-D devices, requiring SVX II-COT track matching in the r - z view is a new possibility. To demonstrate this new capability, we need to show that the r - z track match can be made reliably despite the following potential problems:

- **Ambiguities**
Both COT and SVX II are primarily r - ϕ devices. Hence, the stereo relies on the r - ϕ result, in both.
There is an additional ambiguity in the SVX II 90° stereo due to the ganging in the readout.
- The COT resolutions in r - z and r - ϕ are very different:

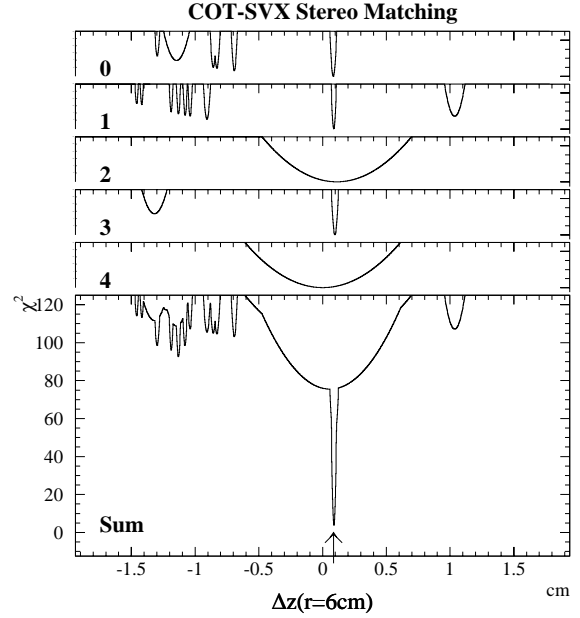


Figure 7.11: Hits in each of SVX II five layers within the 2 cm window, plotted is $\delta(z)$ weighted by the χ^2 , and their sum.

- ~ 0.5000 cm COT extrapolation in r - z
 - ~ 0.0500 cm COT extrapolation in r - ϕ
 - ~ 0.0050 cm SVX II resolution in either view
- As a result, the mis-match between the two detectors is much worse in the stereo view.

For these reasons stereo linking of COT to SVX II is more challenging, and was investigated in detail.

The outline of the algorithm used is as follows:

- Assume a 3D COT track has been found, as described in Sec. 7.4.3.
- Assume that correct SVX II axial hits have been identified, as in previous section.
- For each silicon layer, combine z-strip or small angle stereo clusters with COT helix (1C fit), obtain z , χ^2 .
- Each silicon hit defines a histogram of χ^2 vs z .
- Combine all hits in a layer as

$$\chi_{\text{layer}}^2(z) = \max_{\text{hits}} \chi_{\text{hit}}^2(z)$$

(see the upper 5 histograms in Figure 7.11).

- Combine layers as

$$\chi_{\text{total}}^2(z) = \sum_{\text{layers}} \chi_{\text{layer}}^2(z)$$

(see Figure 7.11 the bottom histogram).

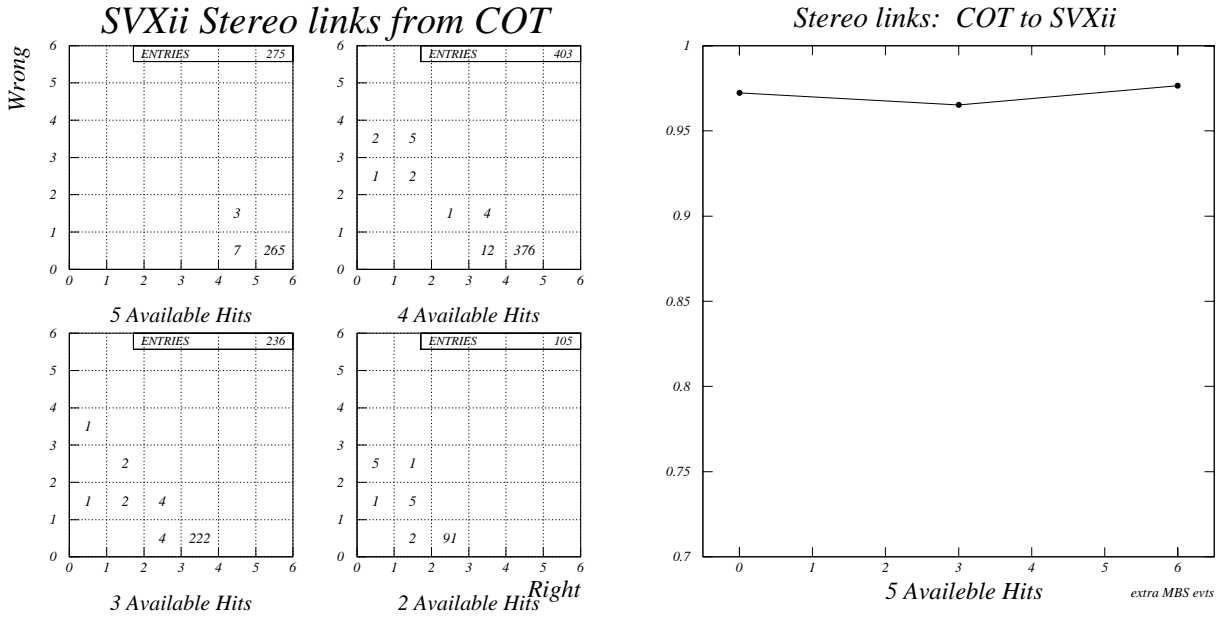


Figure 7.12: Left: Wrong hits linked to COT track vs. right hits, for four cases: 5,4,3, and 2 available hits found in SVX II. Right: Efficiency of linking stereo SVX II hits to COT tracks as a function of luminosity

- Find z with smallest χ^2_{total}

Figure 7.11 illustrates this procedure for one track. The histograms labeled 0 to 4 correspond to the five SVX II layers. Layer 0 is the inner most. Layers 2, and 4 are the small angle stereo - with worse resolution. The histogram labeled sum, combines all the hits in all five layers. The correct hits will have the same z solution and a low χ^2 , and hence have a minimum in this histogram. This approach is fast, because re-fitting is not required for every hit within the road.

For each COT track used, we know from the simulation what the correct hit assignment is. We counted the number of times a wrong hit (i.e. a hit generated by another track, or a noise hit) was linked to the seed COT track. The results are shown on the left in Figure 7.12). The performance of the algorithm on a sample of top events at various luminosities is shown on the right of Figure 7.12. The stereo linking efficiency between COT and SVX II is high, and, within the statistics of this study, shows no degradation up to $N = 6$ overlapping minimum bias events.

7.6.3 COT+SVX II+ISL Resolution

In order to study the resolution of the integrated COT+SVX II tracking system, we assumed that the

hits in the SVX II+ISL have been found. Tracks in the SVX II+ISL were formed by smearing of the ideal helix parameters, using the SVX II+ISL covariance calculated with a single hit resolution of $20\mu\text{m}$. We combined this with the COT helix and covariance to perform a global fit.

The left plot in Figure 7.13 shows the helix parameter resolution for the combined COT+SVX II+ISL fit. The combined system results in $\sim 30\mu\text{m}$ resolutions for both d_0 and z_0 . The right plot shows that there is only weak dependence of the resolution of the reconstructed helix on instantaneous luminosity.

In Figure 7.14 the curvature resolution is translated into $\delta p_T/p_T^2$ as a function of p_T for three luminosities.

7.6.4 Conclusions

We have studied the expected performance of the CDF II tracking upgrades using simulation tools tuned to the similar systems used in CDF during Run I. We find

- The COT reconstruction is highly efficient and gives helix parameter resolutions comparable to what we would expect for the CTC, up to the full Run II design luminosity of $2 \times 10^{32} \text{cm}^{-2} \text{s}^{-1}$.

COT-SVXii Resolutions: Top b -daughters \times COT-SVX Resolution Vs. Luminosity

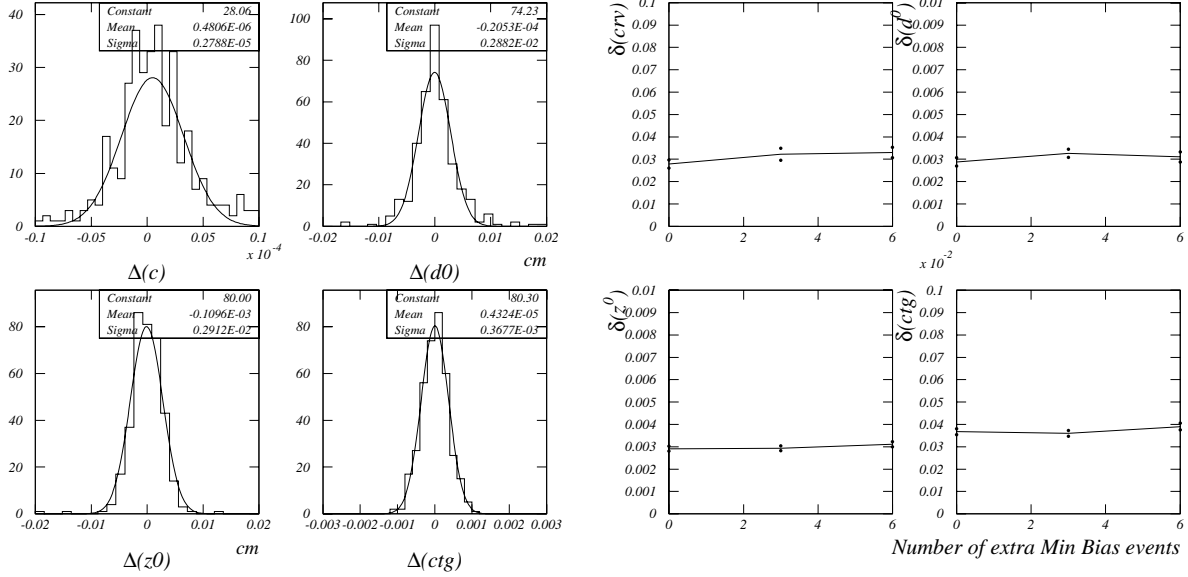


Figure 7.13: Left: Helix parameter resolution for COT+SVX II at low luminosity (the scale of the abscissa is expanded with respect to that used in Figure 7.1). Right: Helix parameter resolutions vs. luminosity

- Track finding in the SVX II+ISL inner tracking system will be efficient, and yield stand-alone silicon track segments with good signal to noise ratio over the full region $|\eta| \leq 2.0$. For tracks with $1.0 \leq |\eta| \leq 2.0$, the seven silicon layers will provide helix parameter resolution adequate to extend electron and muon identification to the plug and IMU, and to allow efficient stand-alone b -tagging.
- The stand-alone SVX II+ISL track segments can be linked to the COT with high efficiency, and the full tracks have excellent helix parameter resolution, comparable to that of the CTC + SVX in Run I. The efficiency and resolution are maintained up to a luminosity of $2 \times 10^{32} \text{ cm}^{-2} \text{ s}^{-1}$.
- The ability to find stand-alone silicon segments over the region $|\eta| \leq 2.0$ allows the use of a fully integrated tracking strategy, according to the plan and specification of Chapter 3. The excellent performance of the system outlined above is, in part, due to the power of this strategy. We expect that as we gain experience with this system we will learn to raise the efficiency and precision of tracking analyses in Run II far beyond the level achieved in Run I.

COT+SVX Momentum resolution Vs. P_T

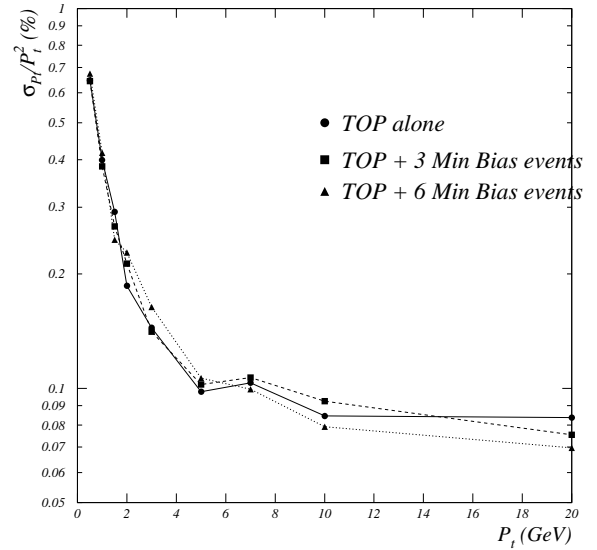


Figure 7.14: Momentum Resolution for COT+SVX II+ISL vs. p_T for three luminosities.